Understanding and Mitigating the Impact of Wi-Fi 6E Interference on Ultra-Wideband Communications and Ranging

Hannah Brunner, Michael Stocker, Maximilian Schuh, Markus Schuß,
Carlo Alberto Boano, and Kay Römer
{hannah.brunner,michael.stocker,schuh,markus.schuss,cboano,roemer}@tugraz.at
Institute of Technical Informatics, Graz University of Technology, Austria

ABSTRACT

The introduction of the Wi-Fi 6E standard operating in the 6 GHz frequency band is a serious threat for IoT systems based on ultra-wideband technology, as they share portions of the same spectrum. Wi-Fi 6E devices can in fact support channel bandwidths up to 160 MHz and operate at a much higher transmission power compared to ultra-wideband devices, which may lead to severe coexistence issues and degraded performance. However, whether and to which extent the performance of ultra-wideband systems worsens due to Wi-Fi 6E interference has not been investigated in detail yet. In this paper, we fill this gap and study how Wi-Fi 6E traffic affects ultra-wideband performance. Our experiments on a large-scale testbed demonstrate that Wi-Fi 6E transmissions may largely disrupt ultra-wideband communications and decrease the accuracy as well as the precision of ranging measurements, with significant consequences on the efficiency of localization systems. We investigate in detail the root causes for the degraded performance and derive empirical observations that can be used to design countermeasures mitigating the impact of Wi-Fi 6E interference. These include, among others, an optimal selection of physical layer settings, as well as the use of a tight synchronization to prevent a false detection of Wi-Fi 6E traffic as ultra-wideband frames and an overshooting of the radio's automatic gain control. We further devise a technique to detect the presence of Wi-Fi 6E traffic and postpone ultra-wideband transmissions accordingly. Our experiments demonstrate that these countermeasures effectively mitigate the impact of Wi-Fi 6E interference on the performance of ultra-wideband systems.

KEYWORDS

Coexistence, Communication, DW1000, Interference, Localization, Performance, Reliability, Testbeds, UWB, Wi-Fi, Wireless.

1 INTRODUCTION

Ultra-wideband (UWB) is one of the most popular RF technologies for the design of location-aware IoT applications [2]. The outstanding time resolution and multipath resilience of UWB radios, combined with their relatively low power consumption, allows the development of decimetre-accurate positioning systems and to support a plethora of application domains, ranging from robot navigation [42] and asset tracking [28] to car access [19] and smart manufacturing [33]. The pervasiveness of UWB systems is expected to increase even further in the coming years, fuelled by the increasing number of UWB manufacturers, by the rising number of start-ups and companies betting on this technology, as well as by the inclusion of UWB transceivers into high-end smartphones.

Coexistence threats on the horizon. Until today, UWB systems have enjoyed a relatively free RF spectrum, as they operate above the crowded 2.4 GHz frequency range on channels that do not overlap with those used by Wi-Fi. For example, the popular Decawave DW1000 transceiver supports six channels in the 3245–7030 MHz range that do not overlap with the portion of spectrum at 5 GHz used by Wi-Fi devices employing IEEE 802.11a/h/j/n/ac/ax. Recently, however, countries and regulatory bodies around the world have started to open the 6 GHz unlicensed band for Wi-Fi use, in connection to the release of the Wi-Fi 6E standard, an extension of IEEE 802.11ax that allows Wi-Fi devices to operate at 6 GHz [15]. Thanks to the additional spectrum capacity, Wi-Fi 6E can support additional channels with larger bandwidths (up to 160 MHz) and unlocks the highest Wi-Fi data speeds, thus enabling mission-critical applications that require higher throughput and lower latencies [65]. Whilst the advent of Wi-Fi 6E represents "a significant milestone for the wireless industry" [15], it is also a serious threat for UWB-based systems, as the latter share the same spectrum and operate at a significantly lower power than Wi-Fi devices. Given the well-known impact that Wi-Fi devices have on low-power wireless systems operating in the 2.4 GHz ISM band [10], it is of utmost importance to (i) study any issues resulting from the coexistence between Wi-Fi 6E and UWB devices, and to (ii) derive countermeasures allowing UWB-based systems to sustain a dependable performance. Unfortunately, to date, whether and to which extent the performance of UWB-based systems is affected by the operations of co-located Wi-Fi 6E devices has not been investigated in detail and on real hardware. Moreover, UWB devices do not have the capability to perform energy detection and hence cannot carry out a clear channel assessment [11]. Unfortunately, most of the existing interference mitigation techniques are based on this prerequisite and thus cannot be applied directly to UWB systems.

Contributions. This paper addresses these gaps and presents the first experimental study analysing the impact of Wi-Fi 6E traffic on the communication and ranging performance of co-located UWB systems based on the popular DW1000 radio.

We start by performing numerous experiments on a large-scale indoor testbed in which UWB and Wi-Fi 6E devices coexist, quantifying the performance of both UWB communications (in terms of packet reception rate) and ranging (in terms of accuracy, precision, and success rate). We do this for different testbed layouts and for various configurations of both Wi-Fi devices (e.g., channel bandwidths, center frequencies, and traffic loads) and UWB nodes (e.g., data rates, payload lengths, preamble symbol repetitions, and other physical layer settings). Our results show, among others, that UWB devices may experience a packet loss up to 96% when two

978-1-6654-9624-7/22/$31.00 ©2022 IEEE
DOI 10.1109/IPSN54338.2022.00015

nearby Wi-Fi stations are streaming a video, that the probability of successfully completing a two-way ranging may be as little as 4% in the presence of Wi-Fi 6E traffic, and that the accuracy and precision of the obtained ranging measurements may also be slightly affected.

We then investigate the root causes for the degraded performance of UWB systems using a mixed signal oscilloscope, which allows us to inspect on a packet level the (in)success of UWB transmissions and the properties of the estimated channel impulse response (CIR) in the presence of colliding Wi-Fi frames. This allows us to shed light on the exact behaviour of UWB systems and to derive empirical observations that we later use to design countermeasures that effectively mitigate the impact of Wi-Fi 6E interference. Such countermeasures include, among others, an optimal selection of physical layer settings and the use of a tight synchronization to prevent a false detection of Wi-Fi 6E traffic as ultra-wideband frames and an overshooting of the radio's automatic gain control.

We further devise a technique to detect the presence of Wi-Fi 6E interference directly on the DW1000 transceiver, and defer UWB transmissions accordingly. Our experiments demonstrate that the use of this scheme, combined with the aforementioned techniques, allows to effectively mitigate the impact of Wi-Fi 6E interference and increase the performance of UWB systems by up to 47%.

Paper outline. We provide background information about UWB and Wi-Fi 6E in § 2. We then present the results from our testbed experiments quantifying the impact of Wi-Fi 6E on the performance of UWB systems in § 3. We analyse the causes for this degraded performance and derive important insights in § 4. Building upon these insights, we enrich UWB devices with several countermeasures to survive Wi-Fi 6E interference and show their effectiveness in § 5. After discussing our work's limitations and the open challenges in § 6, we describe related work in § 7 and conclude the paper in § 8.

2 A PRIMER ON UWB AND WI-FI 6E

We next introduce the UWB and Wi-Fi 6E standards, their main features, and highlight how they share portions of the same spectrum.

2.1 Ultra-Wideband (IEEE 802.15.4a/z)

UWB is a short-range communication technology that uses ns-level pulses and that spreads the signal power over a large bandwidth (≥ than 500 MHz or 20% of the center frequency). This reduces the power spectral density, allows it to resolve individual multipath components, and provides a granular time resolution enabling precise estimations of a signal's time of arrival (ToA). Support for the UWB physical layer (PHY) was formalized by the IEEE 802.15.4a task group in 2007 [34] and evolved into the 802.15.4z standard [37].

Packet structure. An IEEE 802.15.4-compliant UWB packet [35] consists of a *synchronization header* (used for packet detection and channel/ToA estimation) as well as a *data portion*.

Synchronization header (SHR). The SHR contains a *preamble* and a *start-of-frame-delimiter (SFD)* used to indicate the end of the SHR and the beginning of the data modulation. The preamble is built by repeatedly sending the same symbols, and its length is mainly determined by the number of *preamble symbol repetitions (PSR)*. A preamble symbol consists of standard-defined *preamble codes*, i.e., sequences of either 31 or 127 sub-symbols drawn from a ternary alphabet (-1,0,1) corresponding to a positive, absent, or negative

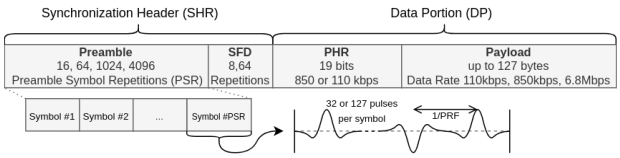

Figure 1: UWB packet structure compliant to IEEE 802.15.4.

pulse, respectively. These pulses are equally spread over ≈ 1μs-long preamble symbols, and the different length of the preamble codes results in different *pulse repetition frequencies (PRF)*, i.e., the rate at which pulses are sent. The SFD is also built from preamble symbols and is 8 or 64 symbols long, depending on the employed data rate. Note that, if a preamble is detected, but an SFD is not received within the expected SHR duration, an SFD timeout is triggered [63].

Data portion (DP). The DP is divided into *physical header (PHR)* and *payload*. While the former contains info about the data length and rate of the upcoming payload, the latter carries the actual data. Unlike the SHR (which is encoded in single pulses), the DP exploits a combination of burst position modulation and binary phase-shift keying. To enhance reliability, error detection/correction codes and a 1/2 bit convolutional encoder are used in the DP [36]. Specifically, the PHR includes a 6-bit parity check enabling single bit error correction and dual bit error detection, whilst the payload uses a Reed-Solomon (RS) encoder appending 48 parity bits every 330 bits of data. Uncorrectable errors in the DP trigger data decoding errors.

PHY settings. UWB radios allow to configure several PHY settings for fine-tuning communication performance. For example, the popular DW1000 radio allows to configure, among others, the DR, PRF, frequency channel, transmission power, and the number of PSR.

Preamble symbol repetitions (PSR). Although the IEEE 802.15.4 standard defines four PSR values (16, 64, 1024, and 4096), the DW1000 radio does not support a PSR of 16 and allows to select additional values (e.g., 128, 256, and 512). Note that a high PSR increases the reliability of the SHR, but at a price of a high energy expenditure [26].

Data rate (DR). The DR defines at which rate the bits of the payload section are transmitted. This value influences the length of each symbol (and, therefore, the length of a packet), as well as the length of the SFD and the DR at which the PHR is sent. Although the IEEE 802.15.4 standard supports DR up to 27 Mbps, the DW1000 radio only supports 110 kbps, 850 kbps, and 6.8 Mbps [16].

Pulse repetition frequency (PRF). The PRF defines the mean rate at which pulses are sent. The PRF of the DP must align with that of the preamble: thus, setting the PRF affects the choice of preamble code. The DW1000 radio only supports a PRF of 16 MHz and 64 MHz.

Frequency channel. The standard defines 16 channels in the sub-GHz band, the low-band (3 – 4.5 GHz), and the high-band (6 –10 GHz) [32]. In this work, we focus on channels 5 and 7 (both supported by the DW1000). These channels have a center frequency of 6489.6 MHz, and a bandwidth of 499.2 and 1081.6 MHz, respectively.

Transmission power (TX power). There are two main regulations dictating the TX power of a UWB radio [1]: the maximum mean power spectral density (which is limited to -43.3 dBm/MHz), and the maximum peak power of a single UWB pulse passing through a 50 MHz filter (which is limited to 0 dBm). Consequently, the chosen DR and PRF affect the maximum TX power of UWB systems. The DW1000

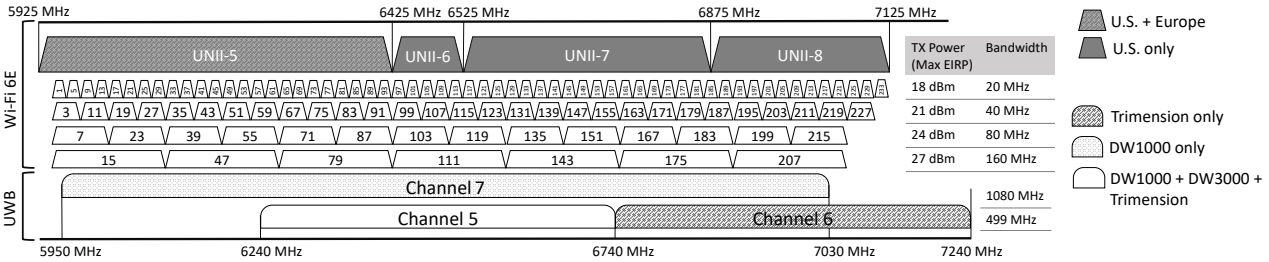

Figure 2: Overview of the (overlapping) channels employed by Wi-Fi 6E and UWB devices operating in the 6 GHz band.

radio offers also a "smart TX power control" feature (`SmartTX`), which allows to increase the TX power within regulatory limits when sending short packets with a DR of 6.8 Mbps [17].

Packet detection and ToA estimation. To detect a packet, coherent UWB radios cross-correlate the received preamble signal with a local template signal generated from the preamble code. The cross-correlation of these two signals $h_s(t)$ is an estimate of the channel impulse response (CIR), which embeds the multipath propagation characteristics of the wireless channel between transmitter and receiver. The DW1000 radio cross-correlates the received preamble signal in chunks of multiple preamble symbols (8, 16, or 64), and the number of symbols per chunk can be configured via the *preamble acquisition chunk (PAC)* register [17]. The ToA is estimated in two steps: first, the radio performs a cross-correlation when searching for the SFD. Then, the receiver uses several channel estimates $h_s(t)$ and sums them up to produce a final CIR estimate $h_c(t)$. The ToA is further refined by analysing $h_c(t)$ and identifying the direct path component (i.e., the first peak of the CIR in line-of-sight conditions).

2.2 Wi-Fi 6E (IEEE 802.11ax)

From its creation in 1999, the IEEE 802.11 specification has been subject to major advancements over the years and evolved into its latest version IEEE 802.11ax [40], also known as Wi-Fi 6. Originally developed for the 2.4 and 5 GHz bands, this standard was recently extended to operate at 6 GHz, as countries and regulatory bodies started to open the corresponding frequencies for unlicensed use. This version of Wi-Fi, referred to as Wi-Fi 6E, offers additional contiguous spectrum of up to 1200 MHz, allowing high-throughput and low-latency communication in yet uncongested bands [65].

Wi-Fi 6E supports channel bandwidths (BW) of 20, 40, 80, or 160 MHz between 5.925 GHz and 7.125 GHz (in the U.S.) or between 5.925 GHz and 6.425 GHz (in Europe), as illustrated in Fig. 2. Wi-Fi 6E defines different access classes to account for power regulations in certain frequency bands to avoid harmful interference with incumbent technologies, as further described in § 2.3. Following these rules, an indoor access point (AP) is allowed to use a TX power between 18 and 27 dBm, depending on the employed channel BW, as shown in Fig. 2. Wi-Fi 6E offers features such as multi-user multiple input multiple output (MU-MIMO) and multi-user orthogonal frequency division multiple access (MU-OFDMA) to improve channel access and spatial re-use. It further introduces a faster modulation scheme of 1024-QAM (Quadrature Amplitude Modulation) to enhance throughput. These features can be exploited especially in the 6 GHz band, where legacy devices do not slow down communication, yielding a theoretical data rate of up to 9.6 Gbps. To ensure backward compatibility, Wi-Fi 6E uses CSMA/CA for channel access and a frame structure akin to previous 802.11 versions [12, 40].

2.3 Coexistence in the 6 GHz Band

In the US, the 6 GHz band is divided into four sub-bands, referred to as U-NII-5 to U-NII-8. So far, the U-NII-5/7 bands have been reserved for fixed point-to-point communication (e.g., reliable backhaul links and satellite services), while the U-NII-6/8 bands have been mostly used for mobile television broadcasts [51]. Due to their low TX power, UWB systems – although unlicensed – have also been allowed to operate in these frequencies, with channels spanning across all four U-NII bands. In 2020, the Federal Communications Commission (FCC) opened these bands for unlicensed use, followed by the European Commission releasing the lower 6 GHz band (i.e., U-NII-5) earlier this year [20]. These changes raised concerns by the UWB Alliance [3], as Wi-Fi devices are now also allowed to use the 6 GHz spectrum, potentially introducing harmful interference.

Although the IEEE 802.15.4 specification offers channels also in other frequency bands, modern UWB chips mostly support only a subset of them. For example, the DW1000 radio [16] supports six different channels: four (1–4) in the low-band below 4.5 GHz, and two (5 and 7) in the high-band at 6489.6 MHz. Its successor, the DW3000 radio [18], instead, shifts towards higher frequencies and supports only channel 5 (at 6489.6 MHz) and 9 (at 7987.2 MHz). A similar trend can be seen on the NXP Trimension [52], which supports channel 5, 6 (at 6988.8 MHz), 8 (at 7488.0 MHz), and 9.

As shown in Fig. 2, channels 5, 6, and 7 are located in the 6 GHz band and share the same frequencies used by Wi-Fi 6E. Notably, due to their wide BW, UWB channels have a spectral overlap with many Wi-Fi 6E channels at once. For example, UWB's channel 5 overlaps with four out of the seven Wi-Fi 6E channels with a 160 MHz BW, whereas UWB's channel 7 overlaps with *all of them*. Simply configuring UWB and Wi-Fi 6E channels such that they use non-overlapping channels is hence hard, especially in the presence of several co-existing networks. It is hence crucial to verify experimentally whether there are any coexistence issues, especially given the low TX power of UWB radios. To the best of our knowledge, however, there has been no study yet investigating the performance of UWB systems in the presence of co-located Wi-Fi 6E devices.

3 IMPACT OF WI-FI 6E ON UWB

In this section, we investigate experimentally whether and how Wi-Fi 6E traffic affects the performance of UWB communication (§ 3.2), ranging (§ 3.3), and localization (§ 3.4). To this end, we set up a testbed facility where UWB and Wi-Fi 6E devices coexist (§ 3.1).

3.1 Testbed Facility

We run our experiments in a testbed facility consisting of 36 UWB nodes deployed in an office building over an area of roughly 270 m^2. Coloured squares mark the location of the UWB nodes in Fig. 3: orange nodes are deployed across a large hallway, whereas green nodes are located inside a 25m^2 office. We will refer to these two configurations as HALLWAY and OFFICE, respectively. All nodes are mounted on a rail at 2.7 m height from the ground. The UWB devices are Decawave `MDEK1001` boards embedding a DW1000 radio, and are connected to Raspberry Pi 4B boards providing power, remote reprogramming, and the ability to collect diagnostic data and logs. The testbed also includes five Qualcomm QCN9074 modules on top of DR6018 v4 boards (marked as red circles in Fig. 3). We use these devices, which are fully Wi-Fi 6E-compliant, to either generate a bandwidth-limited UDP traffic using the `iperf` tool, or to perform video streaming using multiple (different) clients.

3.2 Impact on Communication

We start by studying the impact that Wi-Fi 6E traffic has on the UWB communication performance. Our investigation aims to answer the following questions:

- Does Wi-Fi 6E traffic lead to an increased packet loss across UWB devices? If so, in what form does the loss manifest (e.g., no reception, SFD timeouts, data decoding errors)?
- How do different kinds of Wi-Fi 6E traffic affect the transmissions of UWB devices?
- How does the impact vary as a function of the employed frequency channel / bandwidth?
- How does the impact vary as a function of the distance between devices and for different indoor environments?
- Is the impact more pronounced when using certain PHY settings? Which settings allow to sustain a better performance?

Experimental setup. We configure one UWB node in the testbed as a sink, and let it periodically broadcast beacon packets at a rate of 8 Hz, while letting the remaining UWB nodes log information about successful and unsuccessful receptions. To study the impact of different PHY settings, we run several combinations of channel, PSR, PRF, DR, PAC, and payload lengths. Tab. 1 summarizes the explored PHY settings: unless otherwise specified, we use the settings in bold and node 16 as a sink. For each experiment, we let the sink node transmit 2500 packets. All experiments are repeated four times, and make use of the DW1000's `SmartTX` feature described in § 2.1. Unless otherwise specified, we configure the Wi-Fi 6E devices to operate at maximum power on channel 111 (i.e., center frequency 6495 MHz and 160 MHz bandwidth). This causes an overlap with both channel 5 and 7 used by the UWB nodes (see Fig. 2).

PHY setting	Value(s)
RF channel	**5**, 7
Pulse repetition frequency	16 MHz, **64 MHz**
Preamble symbol repetitions	64, 128, 256, 512, **1024**
Preamble acquisition chunk	8, 16, 32, or 64 based on PSR [17]
Data rate	110 kbps, 850 kbps, **6.8 Mbps**
Payload length	**16 Bytes**, 125 Bytes

Table 1: UWB PHY settings used in our experiments. The default configuration is highlighted in bold.

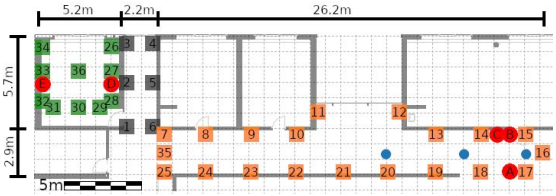

Figure 3: Map of the UWB testbed used in our experimental campaign, which included 36 UWB nodes and five Wi-Fi 6E devices spread over an area of 30×9 m. Red circles identify Wi-Fi devices, whereas orange and green squares mark the position of the UWB nodes in the HALLWAY and OFFICE scenario, respectively.

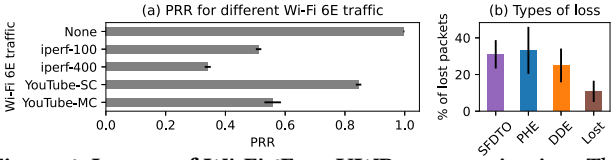

Figure 4: Impact of Wi-Fi 6E on UWB communication. The PRR between UWB nodes in the HALLWAY decreases significantly in presence of Wi-Fi traffic (a). For many of the unsuccessfully received UWB packets, the SHR portion could be partly decoded (b).

Wi-Fi 6E impact. We study the packet reception rate (PRR) of UWB nodes in the absence and presence of Wi-Fi 6E traffic. Given the variable nature of Wi-Fi, we examine different traffic patterns, including bandwidth-limited *periodic* traffic, and *bursty* traffic generated by one or multiple clients. Periodic Wi-Fi 6E traffic is generated using `iperf`, which creates a UDP stream at a fixed bitrate (100 or 400 Mbps) from Ⓑ to Ⓐ. Bursty traffic is generated by streaming a 4K YouTube video from device Ⓐ (serving as AP) to either Ⓑ (single-client scenario) or to both Ⓑ and Ⓒ (multi-client scenario). Fig. 4 (a) shows the average PRR for all UWB nodes in the HALLWAY in the presence and in the absence of Wi-Fi 6E interference. Whilst the PRR is ≈100% in the interference-free scenario, the UWB nodes experience on average a packet loss of about 48% and 65% in the presence of the periodic traffic generated by `iperf` for a bitrate of 100 and 400 Mbps, respectively. The average packet loss when streaming a YouTube video using Wi-Fi 6E is about 16% and 45% for a single client (SC) and for multiple clients (MC), respectively. The differences in PRR trace back to the diverse channel occupancy of periodic and bursty traffic: video streaming is often buffered, and hence creates large white spaces in which UWB transmissions are successful. In contrast, the white spaces left by `iperf` are much shorter, which increases the chances for UWB packets to be hit. As soon as the number of clients grows, the channel occupancy increases drastically, resulting in a significant drop of the PRR.

Fig. 4 (b) depicts how the packet loss manifests at the UWB nodes: interestingly, only a few packets are never received (approx. 10%). In most of the cases, the receiver either experiences a SFD timeout (`SFDTO`), a PHR error (`PHE`), or a data decoding error (`DDE`), which indicates that (portions of the) SHR could be decoded successfully.

Wi-Fi 6E impact across the 6 GHz band. Using the same setup, we study the impact of Wi-Fi 6E traffic on UWB communication performance for HALLWAY nodes as a function of different channel and BW configurations. In this and the following analyses, we focus on periodic traffic (`iperf` at 100 Mbps), as this results in a higher

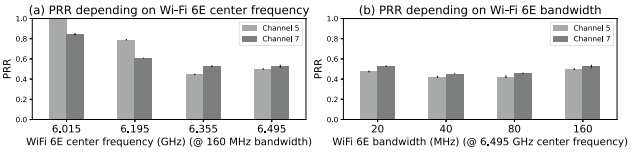

Figure 5: Impact of Wi-Fi 6E on UWB communication for different channel and bandwidth configurations. The use of an UWB channel with a larger bandwidth increases performance only minimally (a). The impact on PRR is severe regardless of the channel bandwidth employed by the Wi-Fi 6E devices (b), leading to a significant packet loss across UWB communications.

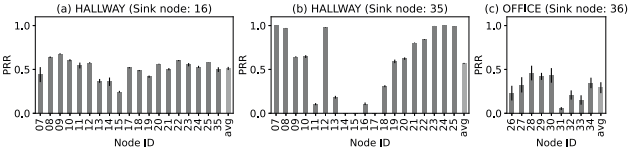

Figure 6: Wi-Fi 6E impact on each UWB node in HALLWAY and OFFICE. In the HALLWAY, UWB nodes in close proximity to a Wi-Fi device exhibit the highest loss, but also the PRR of nodes that are 25 m away from the Wi-Fi device is severely affected (a), (b). In the OFFICE, a Wi-Fi device coexisting with UWB nodes in the same room may cause an almost complete disruption of UWB links (c).

reproducibility and leads to a packet loss that is not as extreme as when streaming a video from multiple clients. Fig 5 (a) shows that the impact of Wi-Fi 6E traffic is, as expected, strongest when making use of frequencies that align with the center of a UWB channel. In such cases (i.e., when using Wi-Fi channel 79 and 111, which overlap with the middle portion of UWB channels 5 and 7), one can see the benefits of using a larger bandwidth: UWB channel 7 (with its 1080 MHz bandwidth) exhibits a slightly better performance than channel 5 (490 MHz bandwidth only). Note that also a partially overlapping Wi-Fi channel affects UWB communication: this can be seen when using Wi-Fi channel 47 (center frequency 6.195 GHz). Fig. 5 (b) further shows that the packet loss is severe regardless of the bandwidth employed by the Wi-Fi 6E devices. Even when using channels with 20, 40, or 80 MHz bandwidth, the average PRR of the HALLWAY nodes decreases below 40%. This is noteworthy, given that the TX power of Wi-Fi 6E decreases with the channel bandwidth, as detailed in § 2.2, and is in line with *theoretical* studies showing that even narrowband interference may harm UWB transceivers [5, 57].

Wi-Fi 6E impact across different locations. We explore how the PRR varies as a function of the distance from the Wi-Fi 6E device(s), and for different environments. Fig. 6 (a) shows that the impact on PRR is more pronounced when an UWB node is in close proximity to a Wi-Fi device (node 15 is 80 cm away from Ⓑ, which is transmitting with `iperf`). Nevertheless, the PRR is low also for UWB nodes that are ≈25 m away from Ⓑ, e.g., node 7, 25, and 35.

We perform the same analysis using node 35 as sink, and present its results in Fig. 6 (b). We can observe that the PRR of the UWB nodes in proximity of Ⓑ drops to zero: this is due to the larger distance from the sink node compared to the previous case. Note that in both figures, non-line-of-sight (NLOS) conditions may contribute to the decrease in PRR: this is particularly visible at node 11.

We further investigate the PRR of the nodes deployed in OFFICE while letting device Ⓔ stream UDP data using `iperf` at 100 Mbps

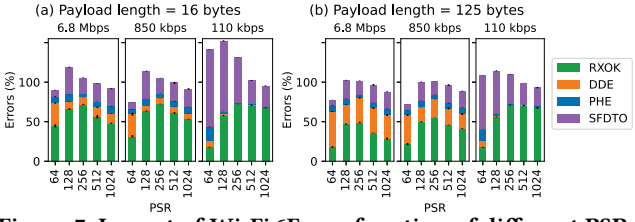

Figure 7: Impact of Wi-Fi 6E as a function of different PSR, DR, and payload lengths (HALLWAY). Very short and long preambles, as well as high DR and long payloads decrease the chances to receive UWB packets in the presence of Wi-Fi 6E traffic.

to Ⓓ. Fig. 6 (c) shows that no node achieves a PRR higher than 46% and that some nodes experience a complete packet loss. This hints that the connectivity between UWB nodes co-located in a small room with a Wi-Fi 6E device may be largely disrupted. Note that the variance in PRR in OFFICE is significantly higher than in HALLWAY.

Wi-Fi 6E impact as a function of different PHY settings. We study how the PRR varies as a function of the different UWB PHY settings introduced in § 2.1 (PSR, DR, PRF, and PAC). To this end, we observe the accumulated errors and distinguish between SFD timeouts (`SFDTO`), occurring when detecting a preamble but not an SFD, PHR errors (`PHE`), occurring when a PHR could not be detected despite the SFD reception, and data decoding errors (`DDE`) due to errors in the DP. Correctly received packets are identified as `RXOK`.

Data rate and preamble length. According to [26], a higher number of PSR increases the reliability of UWB communications: these findings could be confirmed experimentally in our testbed in absence of Wi-Fi 6E traffic. However, the same does not hold true in the presence of Wi-Fi 6E interference. Fig. 7 shows the distribution of accumulated errors and correctly-received packets as a function of different data rates, preamble lengths[1], and payload lengths. The depicted results suggest that a higher number of PSR decreases the probability of a successful packet reception: this is because a longer preamble is more likely to be hit by a Wi-Fi packet. At the same time, also a lower number of PSR decreases the reliability in the presence of Wi-Fi interference. According to Fig. 7, the best performance can be achieved using 256 PSR: the reasons behind this are investigated in § 4. Fig. 7 also hints that a lower data rate (110 kbps) increases the robustness of the data portion and reduces the number of data decoding errors. This better performance, however, comes at a 31× increase in energy consumption, as highlighted in [26]. Another observation is that the sum of `SFDTO`, `PHE`, `DDE`, and `RXOK` is higher than 100%: as detailed in § 4, it seems that the high power of Wi-Fi 6E signals tricks the UWB receiver in believing that there is a preamble even when there is no UWB packet in the air, leading to an SFD timeout. Because of this, an UWB transceiver may unnecessarily remain in listening mode, increasing the energy expenditure. This effect is more pronounced at higher data rates, which might be due to the increased RX sensitivity of these configurations [16].

PRF and PAC size. We finally investigate the role of the PRF and PAC. A higher PRF corresponds to a larger number of pulses transmitted within a symbol (see § 2.1) and is thus considered to increase reliability [26]. Fig. 8 (a) shows that, in the presence of Wi-Fi 6E

[1]Note that, for PSR=64, we employ the register settings proposed in the DW1000 user manual [17], and do *not* make use of the `dwt_configurefor64plen()` API function.

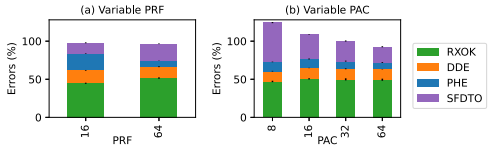

Figure 8: Impact of Wi-Fi 6E interference on UWB communications as a function of different PRF and PAC settings (HALLWAY). The use of a larger PRF and PAC slightly increases the reliability of UWB transmissions in the presence of Wi-Fi 6E traffic.

traffic, increasing the PRF from 16 to 64 MHz leads to an in increase of PRR by 6%. It is worth noting that, due to the limited number of pulses, the TX power is higher when using a PRF of 16 MHz: yet, this configuration yields a worse performance. The chosen PAC does not seem to have an impact on successful packet receptions, as shown in Fig. 8 (b). However, while the PRR is hardly affected, the sensitivity of the receiver increases, resulting in a large number of SFD timeouts and in a large number of *false positives*, i.e., Wi-Fi 6E frames being detected as UWB preambles. In these cases, the receiver is 'locked' to a Wi-Fi 6E packet and might miss actual UWB traffic: the use of a short PAC should thus be avoided.

3.3 Impact on Ranging

We analyse next the impact of Wi-Fi 6E traffic on the UWB ranging process, as well as on the accuracy and precision of the estimated distances. Our investigation aims to answer the following questions:

- Does Wi-Fi 6E traffic affect UWB ranging? If so, what is the likelihood to successfully complete a two-way-ranging in the presence of Wi-Fi 6E interference?
- Is there an impact on the ranging precision and accuracy? If so, how does the impact vary as a function of the number of PSR and of the distance from the interfering Wi-Fi 6E device?

Experimental setup. We let the nodes in the testbed facility described in § 3.1 estimate their distance by performing a single-sided two-way ranging (SS-TWR). We focus on SS-TWR, as this requires the transmission of only two packets and has significantly more chances to successfully complete under Wi-Fi 6E interference than its double-sided counterpart, as discussed next. Specifically, ranging is performed between pairs (I, R) of nodes, consisting of an initiator (I) and a responder (R), where I sends a POLL message, to which R replies with a RESP message. We select pairs of nodes in both HALLWAY and OFFICE, and compare the estimated distances in the presence of Wi-Fi 6E interference to those obtained in absence of it. We quantify how close the distance values are to each other (*precision*) by computing the width of the interval in which 95% of the samples lie, i.e., we compute $P_{95} = Q(0.975) - Q(0.025)$, with $Q(\phi)$ being the ϕ^{th} quantile. We also quantify how close a distance value x is to those measured in absence of interference (*accuracy*) by computing $M_{err} = x - x_m$, where x_m is the median value of the first 100 samples of the first run of experiments in absence of interference. We use the values measured in absence of interference as baseline instead of the true distance between nodes to avoid the introduction of calibration-specific bias in our results. Furthermore, we quantify the *ranging success ratio* $RSR = PRR_{poll} \cdot PRR_{resp}$, where PRR_{poll} and PRR_{resp} are the PRR of the POLL and RESP message, respectively. Note that, unless *both* messages are successfully received, the distance between the two devices cannot be estimated.

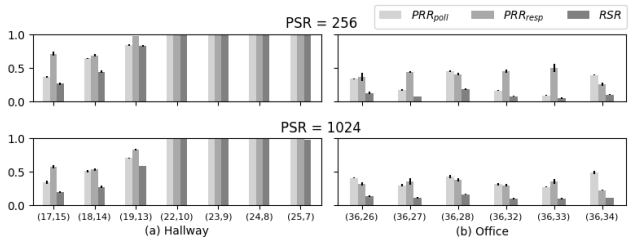

Figure 9: Ranging success ratio in the presence of Wi-Fi 6E interference for HALLWAY (a) and OFFICE (b). The *RSR* is as low as 4% in OFFICE and is 100% in HALLWAY for node pairs that are at more than 15 m distance from the interfering Wi-Fi 6E device.

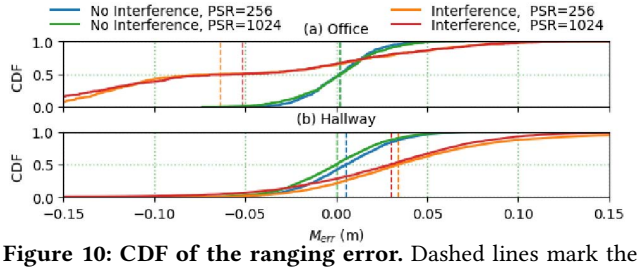

Figure 10: CDF of the ranging error. Dashed lines mark the median error. Wi-Fi 6E traffic increases the error by a few cm.

We study the ranging performance in both OFFICE and HALLWAY. In OFFICE, we perform experiments using node pairs (36,26), (36,27), (36,28), (36,32), (36,33), and (36,34) while Wi-Fi 6E traffic is generated between device Ⓔ and Ⓓ. In HALLWAY, we perform experiments using node pairs (17,15), (18,14), (19,13), (22,10), (23,9), (24,8), and (25,7), while Wi-Fi 6E traffic is generated between device Ⓑ and Ⓐ. All pairs in HALLWAY have the same distance (265 cm): this allows us to analyse how the ranging accuracy and precision varies as a function of the distance from the interfering device. For each pair, we perform 1000 ranging attempts in absence and presence of Wi-Fi interference and repeat each experiment three times. We apply the default PHY settings listed in Tab. 1 and further study the use of two different PSR (256 and 1024). Wi-Fi 6E traffic is generated on channel 111 using `iperf` at 100 Mbps, as described in § 3.2. In absence of Wi-Fi 6E traffic, we observe a *RSR* of 1 for all node pairs.

Wi-Fi 6E impact on ranging success probability. We investigate the ranging success probability and plot in Fig. 9 separately *RSR*, PRR_{poll}, and PRR_{resp} for each pair in both HALLWAY and OFFICE. Fig. 9 shows that the RSR in OFFICE is on average as low as 10% and never above 19%. This shows that when a Wi-Fi 6E device coexists with UWB nodes in a small room, the likelihood to successfully obtain a distance estimate is very low. The pairs in HALLWAY that are in close proximity to device Ⓑ, i.e., (17,15) and (18,14), also exhibit a lower *RSR*, whereas pairs of nodes that are located more than 15 m away can successfully range in almost 100% of the cases. Note that $PRR_{poll} < PRR_{resp}$ for pairs (17,15), (18,14), and (19,13): this is because Ⓑ is closer to the responder node, which lowers the chances to successfully receive a POLL message. Furthermore, the reception of a POLL message allows a node to precisely turn on its radio shortly before the RESP message is sent, practically implementing a synced reception: as we show in § 4, this avoids a gain reduction in the radio's AGC affecting message reception.

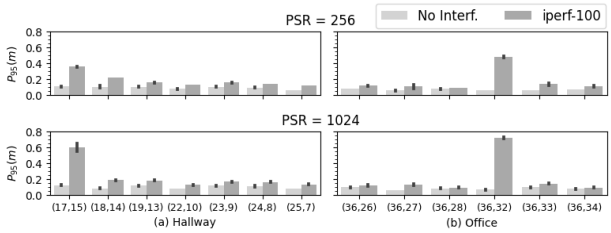

Figure 11: P_{95} interval of the ranging measurements in the absence and presence of Wi-Fi 6E interference. The ranging precision worsens by 10 cm across all nodes under interference and deteriorates especially for pairs in proximity of the Wi-Fi device.

Wi-Fi 6E impact on precision and accuracy. Fig. 10 shows the cumulative error distribution (CDF) of the error (M_{err}, solid lines) as well as the median error (MedE, dashed lines) for HALLWAY and OFFICE pairs in the absence and in the presence of Wi-Fi 6E interference. The MedE is a few cm higher in the presence of Wi-Fi 6E traffic, indicating that the accuracy of the ranging measurements slightly decreases. The MedE between a pair of nodes in the HALLWAY and OFFICE configuration is 3.4 and -6.4 cm, respectively, when using a PSR of 256. Interestingly, the MedE is always positive for hallway nodes far from the Wi-Fi 6E device, but mostly negative for nodes in the office. Furthermore, the maximum ranging error we observed for a *single* measurement amounts to as much as 50 m and 29 m under interference in the HALLWAY and OFFICE (at most 12.3 cm in interference-free experiments), indicating that there may be exceptionally high outliers when ranging under interference.

We further quantify the precision of the ranging measurements in Fig. 11, which shows the P_{95} interval for both HALLWAY and OFFICE for different PSR. When Wi-Fi 6E interference is present, the P_{95} interval increases by ≈10 cm across all nodes, indicating that the precision of ranging worsens compared to the one in absence of interference. Pair (17,15) experiences a particularly high decrease in precision: this is due to the proximity of node 15 to device Ⓑ. However, the precision is even affected at nodes with a distance of more than 15 m from device Ⓑ.

Given the results shown in Figs. 10 and 11, the number of PSR does not seem to play a key role w.r.t. the decrease in ranging accuracy and precision: a shorter PSR yields slightly better results for nodes in very close proximity to Wi-Fi 6E, but the general trends are similar for PSR=256 and 1024.

3.4 Repercussions on Localization Systems

The results shown in § 3.2 and § 3.3 highlight several implications for UWB-based localization systems. In fact, the lower reliability of UWB communications in the presence of Wi-Fi 6E traffic decreases the ranging success probability whenever a node is in close proximity to a Wi-Fi device. Considering that classical localization systems require a tag to carry out a TWR to *several* anchors to unambiguously derive its position, it is very likely that *tens of* attempts are necessary before a position can be computed successfully. This is especially true in smaller rooms like OFFICE, where the RSR is as low as 4% when performing a SS-TWR (Fig. 9), and for alternative TWR schemes that involve the exchange of more messages (such as the DS-TWR). We verify this experimentally by manually placing a tag in both OFFICE and HALLWAY, and by letting it perform a SS-TWR to three surrounding anchors to derive its position (where a successful ranging to all three anchors is needed for an unambiguous estimate). We observe that only 3% and less than 1% of the localization attempts are successful in HALLWAY and OFFICE, respectively – confirming the detrimental effects of Wi-Fi 6E interference on the usability of UWB localization systems based on TWR.

4 ANATOMY OF WI-FI 6E IMPACT ON UWB

In this section, we investigate the impact of Wi-Fi 6E on UWB communication and ranging at a *packet level*, so to gain insights on the root causes for the reduced performance that can be used to derive possible countermeasures. We do this by examining the collisions between Wi-Fi and UWB packets in the time domain using a mixed signal oscilloscope, which allows us to clearly identify the exact portion(s) of UWB packets being hit by Wi-Fi 6E traffic. After introducing the experimental setup (§ 4.1), we show that Wi-Fi 6E traffic affects the reception of UWB packets not only when *colliding* in the air, i.e., when the Wi-Fi and UWB packets overlap partially in time (§ 4.2), but also when being transmitted *shortly before* the arrival of an UWB preamble (§ 4.3). We then analyse how the CIR estimated by UWB radios is affected by the presence of Wi-Fi 6E traffic (§ 4.4).

4.1 Experimental Setup

We place two UWB nodes at 1.8 m distance and let them exchange packets while logging statistics about their reception as well as DW1000-specific information (including the value of several registers and the estimated CIR). We use a Keysight MSO-S 254A mixed signal oscilloscope to capture the exact time interval when UWB and Wi-Fi 6E packets are on the air and save the corresponding traces (see Fig. 13 for an example). By using an RF mixer along with an oscillator, the UWB and Wi-Fi 6E signals in the 6 GHz band are down-converted to satisfy the bandwidth limitations of the oscilloscope and to minimize the amount of collected data.

We pick one UWB node as transmitter and one as receiver: before sending each packet, the transmitter uses a GPIO pin to trigger the receiver (to turn on its radio) and the oscilloscope (to start a measurement). We also use GPIO pins to monitor the DW1000 interrupts [17], so to reveal the time at which preamble and SFD are detected. A Python-based control software configures the UWB modules with given PHY settings, initiates the packet transmissions, and collects/stores the data for later analysis[2].

Wi-Fi 6E traffic is generated using two Qualcomm QCN9074 devices, with the sender placed at ≈ 2 and 3.3 m from the UWB transmitter and receiver, respectively. As it is not possible to precisely schedule the Wi-Fi packet transmissions in time (and thus, to generate collisions with specific portions of the UWB packets), we make use of a brute-force approach in which we let the two Wi-Fi devices continuously exchange data and later post-process the recorded oscilloscope traces to find out whether a collision occurred and in which portion of a UWB packet. The Wi-Fi 6E traffic is generated using `iperf` to create a UDP stream at a fixed 100 Mbps bitrate, as outlined in § 3. We collect more than 48 hours of traces and analyse more than 16000 individual packet transmissions.

[2]The used dataset and scripts are available at https://doi.org/10.5281/zenodo.5602861

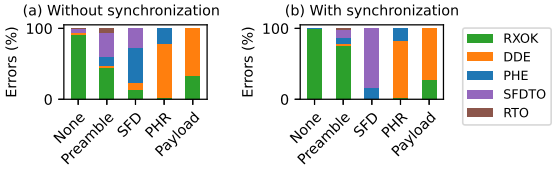

Figure 12: Breakdown of the UWB reception errors depending on the position of the Wi-Fi 6E hit. An UWB receiver is unlikely to recover from a hit in the SFD, PHR, and data portion.

Preamble length (symbols)	64	128	256	512	1024
Recovered packets with single hit in preamble (%)	5.9	27.8	56.4	57.4	61.9
Max. length of preamble hit for recovered packets (µs)	28	93	134	258	396
Packets with multiple hits in preamble (%)	23.0	22.9	26.5	58.4	91.44
Recovered packets with one or more hits in preamble (%)	7.6	41.0	60.7	42.3	27.9

Table 2: Number of hit/recovered UWB packets depending on the preamble length. Although longer preambles allow to recover from a Wi-Fi 6E hit, they are also more likely to be hit multiple times, which results in a lower reception probability.

4.2 Impact of Overlapping Wi-Fi 6E Traffic

We start by investigating the UWB reception errors as a function of the position at which the UWB packet is hit by Wi-Fi 6E traffic. Similar to § 3, we distinguish between SFD timeouts (SFDTO), PHR errors (PHE), data decoding errors (DDE), and correctly-received packets (RXOK). We further consider receiver timeouts (RTO), which refer to packets that are completely missed. Fig. 12 (a) shows the error distribution depending on the position of the Wi-Fi 6E hit for PSR=256 and the other default settings listed in Tab. 1. We observe that some portions of an UWB packet are more robust to interference. While the number of RXOK remains high despite a hit in the preamble, the UWB receiver is more unlikely to recover from a hit in the DP, and almost never receives a packet when Wi-Fi 6E traffic overlaps with SFD or PHR (note: we observe similar trends for other PSR configurations). We discuss next which PHY settings are favourable to 'survive' a Wi-Fi 6E hit in the preamble or in the DP.

The role of the preamble. As observed in our testbed experiments (§ 3), configurations with a long preamble (i.e., with a high number of PSR) exhibit a lower PRR in the presence of Wi-Fi 6E interference. There are two opposing factors leading to this. On the one hand, the longer the preamble, the higher the probability of a collision with Wi-Fi traffic. On the other hand, the UWB receiver is more likely to recover from a Wi-Fi hit when using a long preamble. These trends are supported by Tab. 2, which shows that the UWB receiver is more likely to recover from a *single* Wi-Fi 6E hit and that it can recover even when the Wi-Fi 6E collision is longer. However, depending on the level of interference, the ability to recover from a Wi-Fi 6E hit thanks to a longer preamble may be outweighed by the increased probability of *multiple* Wi-Fi hits. Thus, the total number of recovered packets starts to decline in case of multiple hits. This explains why a PSR of 256 represented the best trade-off in our experiments shown in § 3.2. Consequently, the use of larger preamble sizes is only advisable if Wi-Fi 6E interference is relatively low.

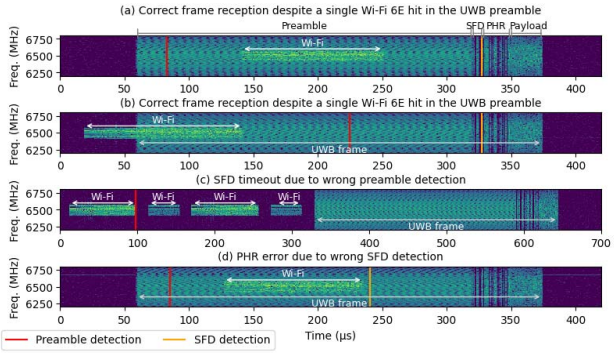

Figure 13: Oscilloscope traces after post-processing and the addition of timing information from the DW1000 receiver. The red and orange bars mark the instant in which the DW1000 receiver detects the preamble and the SFD, respectively. UWB receivers can receive frames despite Wi-Fi 6E hits (a), (b). UWB receivers falsely identify a Wi-Fi 6E frame as a preamble (c) or an SFD sequence (d), which results in a SFDTO or PHE.

The role of the payload. In UWB frames, the DP is encoded using RS codes. As shown in § 3.2, the RS error correction is almost entirely successful for lower data rates (110 kbps). For faster data rates (6.8 Mbps), however, a larger number of data decoding errors occur with increasing payload length. When using a DR of 6.8 Mbps, a payload is sent quickly (i.e., within a minimum of 6 to a maximum of 150 μs). While this is beneficial to avoid collisions, it makes the recovery from Wi-Fi 6E hits unlikely despite the RS error correction. In fact, our experiments reveal that frames experiencing Wi-Fi 6E interference in the DP can only be restored if the packet is hit at the very end of the payload (i.e., within the last 3 µs). Considering that the length of a Wi-Fi 6E frame typically exceeds the length of the UWB data portion, the applicability of error correcting codes is limited: hence, the payload should be kept as short as possible.

4.3 Impact of Non-Overlapping Wi-Fi 6E Traffic

Our experiments also show that even the mere presence of Wi-Fi 6E traffic *before* the transmission of an UWB packet may affect its reception. We identify two main reasons contributing to this effect.

Wi-Fi 6E tricking the UWB decoder. The first problem has already been observed in § 3.2, where for certain PHY settings, the number of reported (and erroneous) receptions exceed the number of actually transmitted packets, indicating that the UWB receiver falsely classifies Wi-Fi 6E packets as UWB preamble symbols. We confirm this assumption by closely monitoring the detection time of preamble and SFD according to the measured DW1000's interrupts. Fig. 13 (c) and (d) show two examples where the UWB receiver wrongly classifies Wi-Fi 6E. In Fig. 13 (c), a Wi-Fi 6E frame is identified as a UWB preamble, resulting in an SFD timeout and a missed UWB packet. In Fig. 13 (d) the UWB receiver detects a valid preamble, but identifies a SFD sequence within the Wi-Fi 6E packet. Hence, a PHR error is triggered and the frame cannot be decoded.

Wi-Fi 6E tricking the AGC. We observe reception errors also if there is neither a collision with Wi-Fi 6E packets nor a misclassification thereof. These cases occur only if a Wi-Fi 6E packet is transmitted *directly before* the UWB preamble. As shown in Fig. 14 (a), the

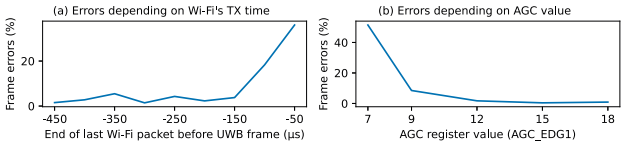

Figure 14: Number of reception errors when Wi-Fi 6E traffic is generated shortly before the UWB packet. The high power of Wi-Fi 6E signals causes the AGC to reduce the gain, leaving the UWB receiver insensitive to incoming frames.

number of reception errors increases the closer the Wi-Fi 6E frame appears before the UWB packet. We identify the DW1000's automatic gain control (AGC) as reason for this behavior. The AGC adjusts the gain of the receiver depending on the perceived signal strength. Due to the high power of Wi-Fi 6E signals, their presence causes the AGC to reduce the gain, thus leaving the UWB receiver insensitive to incoming frames. When observing the DW1000 receiver's AGC status register (`AGC_STAT1`) values, there is indeed a correlation between the status of the AGC and the number of reception errors, as shown in Fig. 14 (b). We will use this correlation in § 5 to detect and mitigate the presence of Wi-Fi 6E traffic.

The benefits of a tight synchronization. To mitigate the aforementioned problems, we introduce a tight synchronization between UWB transmitter and receiver. Using the setup described in § 4.1, we let the transmitter use its GPIO pins to inform the receiver about upcoming UWB frames, such that the latter turns on its radio t_{sync} *before* the expected UWB frame. Fig. 12 compares the reception errors in case of tight ($t_{sync} = 20\mu s$) and loose synchronization ($t_{sync} = 800\mu s$). A tight synchronization clearly allows to eliminate the reception errors due to non-overlapping Wi-Fi 6E traffic, as the latter is no longer falsely detected as UWB frames. Additionally, the number of reception errors in case of a Wi-Fi 6E hit in the preamble decreases. As a tight synchronization does not allow the AGC to react to these Wi-Fi 6E packets early, the receiver sensitivity remains high and a packet reception is rather likely despite a Wi-Fi 6E hit.

4.4 Impact of Wi-Fi 6E on the Estimated CIR

The CIR estimate is used to derive the ToA and is thus crucial for the ranging process (see § 2.1). The DW1000 radio offers several diagnostic registers to assess the quality of the CIR, including the maximum peak amplitude (`PA`), i.e., the maximum amplitude in the CIR estimate, and the total CIR power (`PCIR`), i.e., the sum over the squared samples of the CIR. We study how these indicators are affected under Wi-Fi 6E traffic, as a low-quality CIR estimate may be the reason for the decreased ranging accuracy observed in § 3.2. We use the setup described in § 4.1, and examine `PCIR` and `PA` as a function of the time in which an UWB frame is hit, as shown in Fig. 15 (a). We consider only correctly-received frames (`RXOK`), as SS-TWR requires the reception of both `POLL` and `RESP` messages.

Impact of overlapping Wi-Fi 6E traffic. When Wi-Fi 6E hits the preamble, two different trends can be observed and associated with the scenarios depicted in Fig. 13 (a) and (b). In the first case, the Wi-Fi 6E collision occurs in the beginning of the UWB frame, such that the preamble detection is delayed. In Fig. 15 (a), these cases are indicated by lighter colors, as the color corresponds to the time of the preamble detection event. If the preamble detection is delayed

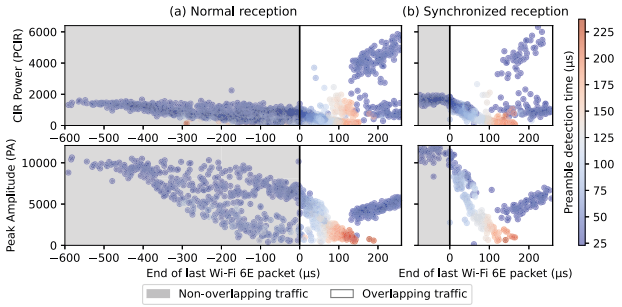

Figure 15: Impact of overlapping and non-overlapping Wi-Fi 6E traffic on key CIR properties. `PCIR` and `PA` decrease when Wi-Fi 6E traffic is present before or during the beginning of an UWB frame, and increase if Wi-Fi 6E hits the preamble later on.

(lighter color), the UWB receiver can accumulate only a limited number of preamble symbols, resulting in a decreased `PA` and `PCIR`. The effect is stronger if the end of the Wi-Fi 6E hit comes later, as this time directly correlates with the number of missed preamble symbols. We assume that a decrease of `PA` and `PCIR` affect the quality of the ToA estimation, as it impedes the identification of the CIR's first peak. Once the end time of a Wi-Fi 6E frame exceeds a certain limit, an opposite trend can be observed, and corresponds to the scenario depicted in Fig. 13 (b). There, a Wi-Fi 6E packet occurs *after* the UWB receiver has detected a valid preamble. The receiver thus starts to cross-correlate and sum up preamble symbols as well as the interfering Wi-Fi 6E frame. As a consequence, `PCIR` increases significantly, hinting that the CIR estimate (and thus the ranging process) might be distorted.

Impact of non-overlapping Wi-Fi 6E traffic. The CIR properties are also affected if there is no actual collision. `PA` and `PCIR` start to decrease even if Wi-Fi 6E traffic ends more than 400 μs before the UWB transmission. Similar to § 4.3, we suspect the DW1000's AGC to be the cause, and introduce a tight synchronization to mitigate the negative impact of non-overlapping Wi-Fi 6E traffic. As shown in Fig. 15 (b), a synchronization does not only allow to avoid a decrease of `PA` and `PCIR` if Wi-Fi 6E traffic occurs before UWB, but also when Wi-Fi 6E hits the beginning of the UWB frame.

5 DEALING WITH WI-FI 6E INTERFERENCE

Based on the insights derived in § 4, we propose and implement next some countermeasures that help to effectively mitigate the impact of Wi-Fi 6E traffic, and evaluate their performance experimentally.

Late wake up (`SYNC`). As Wi-Fi 6E traffic occurring shortly before an UWB transmission may cause an overshooting of the AGC and the false detection of Wi-Fi frames as UWB preambles (§ 4.3), a first simple countermeasure consists in letting the UWB receiver wake up just in time to receive the sent message. To this end, we develop a synchronization scheme between the UWB nodes in our testbed. Specifically, we let the sink node transmit messages in a strictly periodic fashion using a pre-defined interval. The receiver nodes, aware of this interval, make use of the superior time resolution of UWB to wake-up just before the packet is on the air. After receiving the first packet, the receivers derive a timestamp indicating when the next transmission is expected, and continuously refine its value

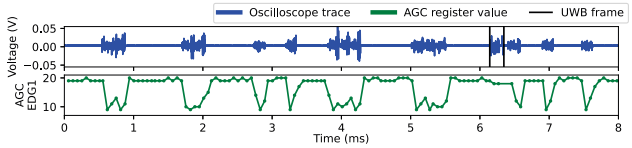

Figure 16: Oscilloscope trace of Wi-Fi 6E traffic and corresponding AGC_STAT1 register values. The AGC_EDG1 value can be used to detect ongoing Wi-Fi 6E traffic.

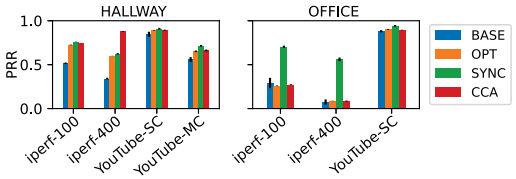

Figure 17: Effectiveness of the proposed countermeasures against Wi-Fi 6E interference for UWB communication. SYNC is most effective in OFFICE; CCA improves the PRR especially in HALLWAY. The improvements depend on the type of Wi-Fi 6E traffic.

at each subsequent message reception, so to account for clock drifts. This approach can easily be integrated into existing TDMA-based protocols, given that a tight synchronization is possible.

Detecting Wi-Fi 6E traffic & deferring transmissions (CCA). The large majority of UWB frames hit by Wi-Fi 6E traffic result in a reception error (§ 4.2). It is hence crucial to detect and avoid Wi-Fi 6E collisions. In traditional wireless protocols, this can be accomplished by performing a clear channel assessment (CCA), i.e., by measuring the energy at the antenna pins, and by comparing it with a given threshold. Unfortunately, the energy detection feature that is typically used to implement CCA functionality on IEEE 802.15.4 narrowband transceivers *is not available* on UWB radios [11]. However, we have noted a correlation between the AGC status register and the presence of Wi-Fi 6E traffic in § 4.3 (see Fig. 14), and we can exploit it to detect and avoid overlapping Wi-Fi 6E traffic. Specifically, we use the AGC_STAT1 register to estimate the energy on the channel before a transmission. Although a single estimation takes $\approx t_{AGC} = 70\mu$ s, the register values clearly allow to detect Wi-Fi 6E activity, as depicted in Fig. 16, and have two nice properties. First, the detection of Wi-Fi 6E traffic is reliable even at large distances (e.g., when there are > 20 m between UWB receiver and Wi-Fi device). Second, UWB frames hardly affect the value (note the black lines in Fig. 16), i.e., one does not mistake UWB activity for Wi-Fi 6E traffic. Consequently, we let an UWB transmitter sample the AGC_STAT1 register n_{CCA} times, compare its value against a threshold CCA_{thr}, and defer transmissions until either n_{CCA} is reached, or until any detected Wi-Fi 6E activity has ceased.

Selecting optimal PHY settings (OPT). Based on the results in § 3, also an optimal selection of PHY settings and the use of short payload lengths is crucial to mitigate the impact of Wi-Fi 6E interference. We hence make use of PSR=256, PRF=64, and a payload length of 16 bytes, in agreement with the findings presented in § 3.2.

Evaluation of the proposed countermeasures. We reuse the same testbed setup as in previous experiments to check the effectiveness of the proposed countermeasures in HALLWAY and OFFICE.

Impact on communication. We use node 16 (HALLWAY) and 36 (OFFICE) as sink, and compare the PRR of the proposed enhancements (OPT, CCA, and SYNC) to the default configuration shown in Tab. 1 (BASE) in the presence of different sources of Wi-Fi 6E traffic. Note that both CCA and SYNC make use of the same PHY settings employed in OPT. For CCA, we empirically choose $n_{CCA} = 10$, compare the AGC_EDG1 value against $CCA_{thr} = 16$, and use AGC_EDV2 for fine-tuning the detection of ceased Wi-Fi activity. Fig. 17 shows how the proposed countermeasures help improving communication performance. In line with the findings presented in § 3.2, OPT allows to increase the PRR compared to BASE by up to 25% in the HALLWAY, whereas in a challenging OFFICE environment OPT does not bring much of an improvement. In such scenarios where Wi-Fi 6E interference is very harsh (e.g., where nodes are in close proximity to the Wi-Fi 6E AP), we observe that SYNC is the most effective technique. Compared to OPT, the PRR of SYNC increases by up to 47% and 3.5% for OFFICE and HALLWAY nodes, respectively, giving a 5x improvement in some cases. In contrast, CCA is mainly beneficial on nodes that are located far away from the Wi-Fi 6E transmitter, as the avoidance of collisions does not prevent a reception error due to the AGC overshooting. The performance of CCA depends on the type of Wi-Fi traffic: compared to OPT, for HALLWAY nodes, the PRR improves by 28% for iperf-400 traffic. Instead, for iperf-100, YouTube-SC and YouTube-MC, the improvement is only of 2%, 0.2%, and 1%, respectively: this is because in these scenarios the gaps between consecutive Wi-Fi 6E frames are often as short as 350μs. Considering an UWB frame length of almost 300μs and a CCA duration of $t_{CCA} = 70\mu$s, a collision can hardly be avoided, which limits the effectiveness of CCA in these cases. It is worth noting, however, that even for this type of traffic, CCA can be an efficient countermeasure if the packet length (i.e., the PSR) is short enough. For example, our experiments show that CCA with a PSR of 64 improves the PRR by 26% even under iperf-100 interference. We further examine the performance of the proposed countermeasures depending on different TX power settings of the Wi-Fi 6E router in the HALLWAY in presence of iperf-100 traffic. Fig. 18 (a) confirms that OPT, SYNC, and CCA improve the PRR of BASE regardless of the Wi-Fi 6E's signal strength. In Fig. 18 (b) and Fig. 18 (c) we distinguish between group of nodes that are placed at close (nodes 15 and 17), medium (nodes 13 and 19), and far distances (nodes 7, 8, 24, and 25) from the Wi-Fi 6E transmitter to better characterize the performance as a function of the distance from the interference source. In line with the observations in Fig. 17, close nodes profit most from SYNC, while CCA can slightly improve the PRR for nodes at larger distances. Note that CCA improves performance by up to 5% and 19% compared to OPT and BASE, respectively, even if nodes are placed more than 20 m from a Wi-Fi 6E device transmitting with only 8 dBm power: this confirms the effectiveness of our solutions.

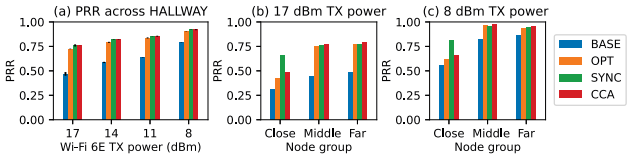

Figure 18: Effectiveness of the proposed countermeasures when varying the TX power of the Wi-Fi 6E device. OPT, SYNC, and CCA consistently help increasing the PRR, especially for UWB nodes deployed in proximity of a Wi-Fi 6E device.

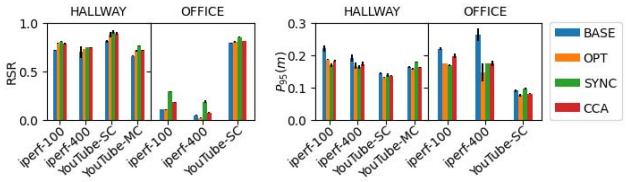

Figure 19: Effectiveness of proposed countermeasures against Wi-Fi 6E interference for UWB ranging. Throughout all configurations, SYNC is most effective in increasing the RSR; OPT is the most effective in decreasing the P_{95} interval.

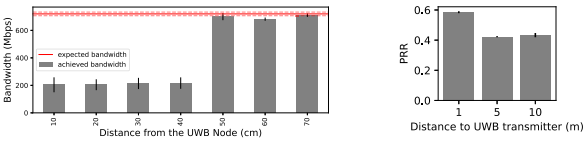

(a) Impact of UWB on Wi-Fi 6E **(b) DW3000 performance**

Figure 20: Impact of UWB transmissions on the reliability of Wi-Fi 6E communications (a) and vulnerability of the DW3000 transceiver to Wi-Fi 6E traffic (b). We can observe that Wi-Fi performance is affected (a) and that also new-generation UWB platforms suffer from Wi-Fi 6E interference.

Impact on ranging. We also apply OPT, SYNC, and CCA to SS-TWR and evaluate the improvements w.r.t. the ranging success probability (RSR) and precision. Note that we apply SYNC and CCA to the POLL message, while the RESP message is implicitly synchronized as explained in § 3.3. Fig. 19 shows the average P_{95} interval and RSR for all OFFICE pairs and HALLWAY pairs (17,15), (18,14), (24,8) and (25,7). In line with our previous observations, OPT allows to improve the RSR in HALLWAY by up to 7% compared to BASE, whilst the highest improvements on RSR brought by SYNC are found in OFFICE (up to 18% improvement compared to OPT). Interestingly, CCA is more effective in OFFICE, where it gives an improvement of up to 9%.

In HALLWAY, the performance of CCA is mainly limited due to the experimental setup, i.e., the majority of node pairs experience a high RSR by default. In OFFICE, the increased RSR is based on a high PRR_{resp}, which might result from a time-dependency between the POLL message, the RESP message, and the Wi-Fi 6E traffic pattern. Exploiting these dependencies to further increase RSR is an interesting direction for future work, but outside the scope of this paper. Finally, we also observe that OPT allows to improve the ranging precision compared to BASE by up to 18% and 46% in HALLWAY and OFFICE, respectively (for a PSR of 256, the P_{95} interval decreases by up to 4 and 12 cm). SYNC and CCA generally improve performance compared to BASE, but none of the approaches seems to consistently outperform OPT on all different configurations. We will carry out further studies on how to compensate the ranging errors induced by Wi-Fi 6E interference in future work.

6 DISCUSSION AND FUTURE WORK

Is Wi-Fi 6E affected by UWB? In this work, we have focused on the impact of Wi-Fi 6E on UWB systems. However, it is also important to verify whether UWB traffic affects the performance of co-located Wi-Fi devices, especially since IEEE 802.15.4 narrowband devices are known to affect Wi-Fi's performance in the 2.4 GHz band

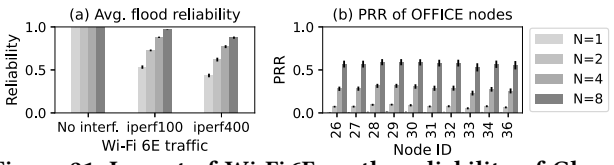

Figure 21: Impact of Wi-Fi 6E on the reliability of Glossy. Average reliability of a flood throughout the testbed (a), and PRR on OFFICE nodes for `iperf400` (b). N denotes the # of flood repetitions.

when transmitting in close proximity [43]. During our experiments, we have observed that UWB transmissions do actually affect the reliability of Wi-Fi 6E communications. Fig. 20a shows that Wi-Fi 6E devices may experience a degradation of bandwidth up to 71% when an active UWB node is located less than 50 cm away. We have obtained this data by configuring device Ⓐ to use `iperf-100` for sending UDP traffic towards device Ⓑ, and by manually deploying a UWB node periodically transmitting data at different distances from Ⓑ. The UWB node makes use of the default settings shown in Tab. 1. These preliminary results show that also Wi-Fi 6E devices may suffer coexistence problems due to co-located UWB nodes. Investigating in detail these issues is a promising avenue for future work.

Impact of Wi-Fi 6E on newer UWB hardware. Our experiments have exclusively targeted the popular DW1000 radio. However, the degraded performance in the presence of Wi-Fi 6E traffic is also visible in the new generation of UWB transceivers. Specifically, we quantify the impact on a pair of UWB nodes equipped with a DW3000 transceiver. In this experiment, the transmitter is mounted next to node 16, while the receiver is manually placed at different distances along the HALLWAY, as indicated by blue dots in Fig. 3. The nodes use the default configuration shown in Tab. 1. Fig. 20b shows that in presence of Wi-Fi 6E `iperf-100` traffic (generated between device Ⓐ →Ⓑ), the PRR can be as low as 42%, which is in line with the results in § 3.2. These results hence show that the impact of Wi-Fi 6E traffic is not limited to the ubiquitous DW1000 platform, but also affects newer UWB radios. A detailed investigation of how different hardware platforms are affected by Wi-Fi 6E is not possible due to space constraints and will be investigated in future work.

Concurrent transmissions to the rescue? Recently, a growing number of low-power wireless protocols leveraging the principle of concurrent transmissions (CTX) has achieved unprecedented reliability, latency, and energy efficiency even in harsh RF environments [54, 56]. After being widely applied in the context of IEEE 802.15.4 narrowband systems for reliable and low-latency data collection and dissemination [70], CTX-based flooding has recently found its way in UWB systems [44, 62, 63], showing remarkable performance thanks to the spatial diversity and temporal redundancy of Glossy [22]. It is hence interesting to investigate whether the use of CTX increases the reliability of UWB systems in the presence of Wi-Fi 6E interference, given that they enforce a tight synchronization among nodes, which was shown to be useful in § 4. While a thorough study of the CTX performance goes beyond the scope of this paper, we give a preliminary answer to this question by setting up an experiment as follows. We port the open-source CTX implementation of Glossy for UWB provided by Lobba et al. [44] to the MDEK1001 platform used in our testbed (see § 3.1). We disseminate 8×2500 packets from node 16 to all other nodes

in the testbed (using DR=6.8 Mbps, PRF=64 MHz, PSR=64, channel 5, and a payload length of 16 bytes), and track the reception of packets at each node. Fig. 21 (a) shows the average flood reliability in the entire testbed when generating `iperf` traffic between Ⓑ→Ⓐ and Ⓔ→Ⓓ. The reliability is only ≈ 50% when using a single transmission (N=1) and increases but still does not reach 100% even with several re-transmissions (N=8). Moreover, harsh environments such as OFFICE significantly deteriorate the performance of flooding. Fig. 21 (b) shows that OFFICE nodes receive at most 55% of the packets under `iperf400` despite using N=8. Thus, additional investigations are necessary to harness the full potential of CTX in mitigating the impact of Wi-Fi 6E interference on UWB systems: we will be addressing this in future work.

Performance of concurrent ranging. In this work, we have focused on standard TWR due to its high usage in real-world applications. However, concurrent ranging [14, 25] and the use of quasi-simultaneous transmissions for scalable localization [13, 27] have recently gained popularity in the community. Based on the results shown in § 3 and § 4, these schemes are likely to outperform TWR in the presence of Wi-Fi 6E interference for two reasons. First, they decrease the number of necessary transmissions. Second, they rely more on CIR-related information than on payload data. Given that the SHR can often be decoded despite a Wi-Fi 6E hit (see § 3.2 and § 4.2), these schemes may be less susceptible to interference than TWR. A full investigation of the performance of these schemes is beyond the scope of this paper and will be part of future work.

7 RELATED WORK

The interest of the research community in UWB technology has soared about a decade ago, after the commercialization of the first low-cost UWB transceivers compliant to the IEEE 802.15.4 standard. Since then, a large body of work has proposed algorithms, protocols, and techniques to build robust, scalable, and efficient UWB-based positioning systems that can achieve a cm-level accuracy [2].

Performance of UWB communication & ranging. Several studies have investigated the performance of UWB solutions on real hardware. For example, Lymberopoulos and Liu [45] have benchmarked the localization accuracy of various systems under the same settings, whereas other studies have focused specifically on the performance under NLOS conditions [48, 60]. Many works have also studied the impact of different PHY settings configurations on the performance of both UWB communication [26, 62, 63] and ranging [14, 24, 49, 50]. However, all these studies were carried out in ideal environments *free of harmful interference* for UWB systems.

Coexistence of UWB and Wi-Fi. After the FCC authorized the unlicensed use of UWB in the 3.1–10.6 GHz frequency range [21], it was soon observed that this may lead to coexistence issues with Wi-Fi systems operating at 5 GHz. This triggered several studies simulating the impact of UWB transmissions on IEEE 802.11a networks [5, 39, 47] and of IEEE 802.11a traffic on UWB systems [5, 23], which highlighted that interference can mutually cause a degraded performance. Other studies in the microwave engineering community have proposed adjustments to the transceiver design and the use of non-linear filters to improve UWB performance under narrowband interference [41, 58]. All these works, however, were carried out in simulation under very ideal conditions and targeted UWB before the formulation of the IEEE 802.15.4a standard, which dictates the characteristics of today's UWB transceivers. Moreover, previous studies did not target new Wi-Fi 6E devices but considered first-generation Wi-Fi platforms following the IEEE 802.11a standard, whose characteristics are vastly different. Despite the increasing concerns about the threat posed by Wi-Fi 6E on UWB performance [61], no work has – to the best of our knowledge – quantified the impact of Wi-Fi 6E on today's off-the-shelf UWB hardware yet. Our study is hence the first work filling this gap.

Wi-Fi interference vs. low-power wireless systems. After the first measurements highlighting the increasing congestion in the 2.4 GHz band [29, 53, 69], the low-power wireless networking community has started to deal with the performance degradation caused by co-located Wi-Fi devices. Several techniques were proposed to improve the performance of communication protocols in the presence of external interference [10], ranging from adaptive channel hopping [64, 66], and RSSI-based recovery [30], to adaptive CCA [6, 67], and increased redundancy [7, 43]. Several researchers have also devised techniques to reliably detect and classify interference [31, 59, 68]. Furthermore, in recent years, dedicated tools [8, 56] and competitions [9, 54, 55] have fostered the creation of reliable protocols that can effectively mitigate the presence of Wi-Fi traffic, for example by leveraging concurrent transmissions [4, 38, 46, 70]. However, all these works have focused on the impact of Wi-Fi on IEEE 802.15.4 *narrowband* systems operating in the 2.4 GHz band. We are the first to study the impact of Wi-Fi 6E on IEEE 802.15.4 UWB systems, and the first to propose countermeasures to effectively mitigate it. We also tackle the lack of a CCA feature in UWB radios [11] and propose a technique that achieves a similar purpose, enabling both the detection and mitigation of Wi-Fi 6E interference.

8 CONCLUSIONS

In this paper we provide the first study analysing the impact of Wi-Fi 6E traffic on the performance of co-located UWB systems. After showing the significant degradation of both communication and ranging performance, we analyse the Wi-Fi 6E impact in a fine-grained way and derive a number of insights as well as countermeasures that can be effectively used to mitigate the problem. We believe that our results will raise awareness about the severity of the coexistence problems in the 6 GHz band, and provide novel stimuli to the low-power wireless community to investigate how to further improve the dependability of UWB-based systems.

Acknowledgements. The authors thank Klaus Witrisal and the SPSC lab for borrowing us the oscilloscope and other equipment used in our experiments. This work has been performed within the TU Graz LEAD project "Dependable Internet of Things in Adverse Environments". This work was also supported by the TRANSACT project. TRANSACT (https://transact-ecsel.eu/) has received funding from the Electronic Component Systems for European Leadership Joint Undertaking under grant agreement no. 101007260. This joint undertaking receives support from the European Union's Horizon 2020 research and innovation programme and Austria, Belgium, Denmark, Finland, Germany, Poland, Netherlands, Norway, and Spain. TRANSACT is also funded by the Austrian Federal Ministry of Transport, Innovation and Technology under the program "ICT of the Future" (https://iktderzukunft.at/en/).

REFERENCES

[1] 3db Access AG. 2019. Impulse Radio UWB Principles and Regulation. [Online] https://www.3db-access.com/article/17 – Last access: 2021-10-29.

[2] A. Alarifi et al. 2016. Ultra Wideband Indoor Positioning Technologies: Analysis and Recent Advances. *Sensors* 16, 5 (2016).

[3] Ultra Wide Band (UWB) Alliance. 2019. Comments of The Ultra Wide Band (UWB) Alliance Before The Federal Communications Commission.

[4] M. Baddeley et al. 2020. The Impact of the Physical Layer on the Performance of Concurrent Transmissions. In *Proc. of the 28th ICNP Conf.*

[5] J. Bellorado et al. 2003. Coexistence of ultra-wideband systems with IEEE-802.11 a wireless LANs. In *Proc. of the GLOBECOM Conf.*, Vol. 1. IEEE.

[6] M. Bertocco et al. 2007. Experimental Optimization of CCA Thresholds in WSNs in the Presence of Interference. In *Proc. of the EMC Workshop*. IEEE.

[7] C.A. Boano et al. 2010. Making Sensornet MAC Protocols Robust Against Interference. In *Proc. of the 7th EWSN Conf.* Springer.

[8] C.A. Boano et al. 2011. JamLab: Augmenting Sensornet Testbeds with Realistic and Controlled Interference Generation. In *Proc. of the 10th IPSN Conf.*

[9] C.A. Boano et al. 2017. EWSN Dependability Competition: Experiences and Lessons Learned. *IEEE Internet of Things Newsletter* (2017).

[10] C.A. Boano and K. Römer. 2013. External Radio Interference. In *Radio Link Quality Estimation in Low-Power Wireless Networks*. Springer.

[11] M. Charlier et al. 2019. Challenges in Using Time Slotted Channel Hopping with Ultra Wideband Communications. In *Proc. of the 4th IoTDI Conf.* ACM.

[12] Cisco. 2021. Wi-Fi 6E: The Next Great Chapter in Wi-Fi. [Online] https://tinyurl.com/vv2ttc9v – Last access: 2021-10-29.

[13] P. Corbalán et al. 2019. Chorus: UWB Concurrent Transmissions for GPS-like Passive Localization of Countless Targets. In *Proc. of the 18th IPSN Conf.* ACM.

[14] P. Corbalán and G.P. Picco. 2020. Ultra-wideband Concurrent Ranging. *ACM TOSN* 16, 4 (2020).

[15] E. Danel. 2020. An Introduction to Wi-Fi 6E Spectrum in the 6 GHz band. [Online] https://tinyurl.com/5xpmy9re – Last access: 2021-10-29.

[16] Decawave. 2015. DW1000 Datasheet, version 2.09. [Online] https://tinyurl.com/3wyyefrp – Last access: 2021-10-29.

[17] Decawave. 2017. DW1000 User Manual, version 2.11. [Online] https://tinyurl.com/cmu4unex – Last access: 2021-10-29.

[18] Decawave. 2020. DW3000 Datasheet, version 1.1. [Online] https://tinyurl.com/2ddkv44z – Last access: 2021-10-29.

[19] EETimes. 2019. VW and NXP Show First Car Using UWB To Combat Relay Theft. [Online] https://tinyurl.com/201ybh88y5e – Last access: 2021-10-29.

[20] European Union. 2021. Decision on the Harmonised Use of Radio Spectrum in the 5945–6425 MHz Band. [Online] https://bit.ly/3mTOPtc – Last access: 2021-10-29.

[21] Federal Communications Commission. 2002. First Report and Order (FCC 02-48). [Online] https://tinyurl.com/9rukj5k9 – Last access: 2021-10-29.

[22] F. Ferrari et al. 2011. Efficient Network Flooding and Time Synchronization with Glossy. In *Proc. of the 10th IPSN Conf.* IEEE.

[23] B. Firoozbakhsh et al. 2003. Analysis of IEEE 802.11a Interference on UWB Systems. In *Proc. of the UWBST Conf.* IEEE.

[24] T. Gigl et al. 2012. Ranging Performance of the IEEE 802.15.4a UWB Standard Under FCC/CEPT Regulations. *JECE* (2012).

[25] B. Großwindhager et al. 2018. Concurrent Ranging with UWB Radios: From Experimental Evidence to a Practical Solution. In *Proc. of the 38th ICDCS Conf.*

[26] B. Großwindhager et al. 2018. Enabling Runtime Adaptation of PHY Settings for Dependable UWB Communications. In *Proc. of the 19th WoWMoM Symp.* IEEE.

[27] B. Großwindhager et al. 2019. SnapLoc: An Ultra-Fast UWB-Based Indoor Localization System for an Unlimited Number of Tags. In *Proc. of the 18th IPSN Conf.*

[28] A. Gupta. 2018. *Development of UWB-IR based Low Power Asset Tracking System with Precise Location Information.* Master's thesis. NTU, Singapore.

[29] J. Hauer et al. 2009. Experimental Study of the Impact of WLAN Interference on IEEE 802.15.4 Body Area Networks. In *Proc. of the 6th EWSN Conf.* Springer.

[30] J. Hauer et al. 2010. Mitigating the Effects of RF Interference through RSSI-Based Error Recovery. In *Proc. of the 7th EWSN Conf.* Springer.

[31] F. Hermans et al. 2013. SoNIC: Classifying Interference in 802.15.4 Sensor Networks. In *Proc. of the 12th IPSN Conf.* IEEE.

[32] E. Hsu. 2021. An Overview of the IEEE 802.15.4 HRP UWB Standard. [Online] https://tinyurl.com/2t5htryy – Last access: 2021-10-29.

[33] S. Huang et al. 2017. A Real-time Location System Based on RFID and UWB for Digital Manufacturing Workshop. *Procedia CIRP* 63, 1 (2017).

[34] IEEE 802.15.4 Working Group. 2007. IEEE Standard for Information technology – Local and metropolitan area networks – Part 802.15.4a-2007.

[35] IEEE 802.15.4 Working Group. 2011. IEEE Standard for Local and Metropolitan Area Networks – Part 802.15.4-2011: LR-WPANs.

[36] IEEE 802.15.4 Working Group. 2016. IEEE Standard for Low-Rate Wireless Networks – Part 802.15.4-2015: LR-WPANs.

[37] IEEE 802.15.4 Working Group. 2020. IEEE Standard for Low-Rate Wireless Networks – Part 802.15.4z-2020: Enhanced UWB PHYs and Ranging Techniques.

[38] T. Istomin et al. 2018. Interference-Resilient Ultra-Low Power Aperiodic Data Collection. In *Proc. of the 17th IPSN Conf.* ACM.

[39] N.V. Kajale. 2005. *UWB and WLAN Coexistence: a Comparison of Interference Reduction Techniques.* Master's thesis. University of South Florida, USA.

[40] E. Khorov et al. 2018. A Tutorial on IEEE 802.11ax High Efficiency WLANs. *IEEE Communications Surveys & Tutorials* 21, 1 (2018).

[41] N.F. Krasner. 2017. Interference Mitigation for Positioning Systems. [Online] https://uspto.report/patent/grant/9,971,018 – Last access: 2021-10-29.

[42] A. Ledergerber et al. 2015. A Robot Self-Localization System using One-Way Ultra-Wideband Communication. In *Proc. of the IROS Conf.* IEEE / RSJ.

[43] C.M. Liang et al. 2010. Surviving Wi-Fi Interference in Low Power ZigBee Networks. In *Proc. of the 8th SenSys Conf.* ACM.

[44] D. Lobba et al. 2020. Concurrent Transmissions for Multi-hop Communication on Ultra-wideband Radios. In *Proc. of the 17th EWSN Conf.*

[45] D. Lymberopoulos and J. Liu. 2017. The Microsoft Indoor Localization Competition: Experiences and Lessons Learned. *IEEE Sig. Proc. Mag.* 34, 5 (2017).

[46] X. Ma et al. 2020. Harmony: Saving Concurrent Transmissions from Harsh RF Interference. In *Proc. of the INFOCOM Conf.* IEEE.

[47] S.R. Mallipeddy et al. 2010. Impact of UWB Interference on IEEE 802.11a WLAN System. In *Proc. of the NCC Conf.* IEEE.

[48] S. Maranò et al. 2010. NLOS Identification and Mitigation for Localization Based on UWB Experimental Data. *J-SAC* 28, 7 (2010).

[49] K. Mikhaylov et al. 2017. Impact of IEEE 802.15.4 Communication Settings on Performance in Asynchronous Two Way UWB Ranging. *International Journal of Wireless Information Networks* 24, 2 (2017).

[50] H. Mohammadmoradi et al. 2018. UWB PHY Adaptation for Best Ranging Performance within Appl. Constraints. In *Proc. of the 2nd ICSDE Conf.* ACM.

[51] G. Naik et al. 2020. Next generation Wi-Fi and 5G NR-U in the 6 GHz bands: Opportunities and Challenges. *IEEE Access* 8 (2020).

[52] NXP. 2020. Secure Ultra-Wideband (UWB) Positioning and Ranging optimized for IoT Use Cases. [Online] https://tinyurl.com/9c63rpeu – Last access: 2021-10-29.

[53] M. Petrova et al. 2007. Interference Meas. on Perf. Degradation between Colocated IEEE 802.11g/n and IEEE 802.15.4 Networks. In *Proc. of the 6th ICN Conf.* IEEE.

[54] M. Schuß et al. 2017. A Competition to Push the Dependability of Low-Power Wireless Protocols to the Edge. In *Proc. of the 14th EWSN Conf.*

[55] M. Schuß et al. 2018. Moving Beyond Competitions: Extending D-Cube to Seamlessly Benchmark Low-Power Wireless Systems. In *Proc. of the 1st CPSBench Worskh.*

[56] M. Schuß et al. 2019. JamLab-NG: Benchmarking Low-Power Wireless Protocols under Controllable and Repeatable Wi-Fi Interf.. In *Proc. of the 16th EWSN Conf.*

[57] E.M. Shaheen et al. 2012. Analysis and Mitigation of the Narrowband Interference Impact on IR-UWB Communication Systems. *JECE* (2012).

[58] S. Sharma et al. 2018. Impulse Noise Mitigation in IR-UWB Communication Using Signal Cluster Sparsity. *IEEE Communications Letters* 22, 3 (2018).

[59] L. Stabellini and J. Zander. 2010. Energy-Efficient Detection of Intermittent Interference in Wireless Sensor Networks. *IJSNET* 8, 1 (2010).

[60] M. Stocker et al. 2021. Performance of Support Vector Regression in Correcting UWB Ranging Measurements under LOS/NLOS Conditions. In *Proc. of the 4th CPS-IoTBench Workshop*. IEEE.

[61] C. Swedberg. 2020. FCC's Wi-Fi 6 GHz Plan Poses Interference for UWB. [Online] https://tinyurl.com/2rwhncxy – Last access: 2021-10-29.

[62] M. Trobinger et al. 2020. One Flood to Route Them All: Ultra-fast Convergecast of Concurrent Flows over UWB. In *Proc. of the 18th SenSys Conf.* ACM.

[63] D. Vecchia et al. 2019. Playing with Fire: Exploring Concurrent Transmissions in Ultra-Wideband Radios. In *Proc. of the 16th SECON Conf.* IEEE.

[64] T. Watteyne et al. 2009. Reliability Through Frequency Diversity: Why Channel Hopping Makes Sense. In *Proc. of the 6th PE-WASUN Symp.* ACM.

[65] Wi-Fi Alliance. 2021. Wi-Fi 6E expands Wi-Fi into 6 GHz. [Online] https://tinyurl.com/25uhb3fu – Last access: 2021-10-29.

[66] W. Xu et al. 2008. Defending Wireless Sensor Networks from Radio Interference through Channel Adaptation. *ACM TOSN* 4 (2008). Issue 4.

[67] W. Yuan et al. 2010. Adaptive CCA for IEEE 802.15.4 Wireless Sensor Networks to Mitigate Interference. In *Proc. of the WCNC Conf.* IEEE.

[68] S. Zacharias et al. 2014. A Lightweight Classific. Alg. for External Sources of Interf. in IEEE 802.15.4-based WSNs Operating at the 2.4 GHz. *IJDSN* 10, 9 (2014).

[69] G. Zhou et al. 2006. Crowded Spectrum in Wireless Sensor Networks. In *Proc. of the 3rd EmNets Workshop.*

[70] M. Zimmerling et al. 2021. Synchronous Transm. in Low-Power Wireless: A Survey of Comm. Protocols and Network Services. *ACM Comp. Surv.* 53, 6 (2021).